

Research article

Efficiency of GrowDex® nanofibrillar cellulosic hydrogel when generating homotypic and heterotypic 3D tumor spheroids

Perumalsamy Balaji^{1,4}, Anbazhagan Murugadas^{2,4}, Lauri Paasonen³, Sellathamby Shanmugaapriya¹ and Mohammad A. Akbarsha^{4,5,*}

¹ Department of Biomedical Science, Bharathidasan University, Tiruchirapalli 620024, India [Present address: Department of Biochemistry, University of Nebraska Medical Center, Omaha, Nebraska, USA]

² Department of Environmental Biotechnology, Bharathidasan University, Tiruchirapalli 620024, India [Present address: Department of Pediatrics, Emory University School of Medicine & Children's Healthcare of Atlanta, Atlanta, Georgia, USA]

³ UPM Biomedicals, Helsinki, Finland

⁴ Mahatma Gandhi-Doerenkamp Centre for Alternatives, Bharathidasan University, Tiruchirappalli 620024, India

⁵ National College (Autonomous), Tiruchirappalli 620001, India

* Correspondence: Email: rc@nct.ac.in; Tel: +919790995854.

Abstract: In recent times, homotypic and heterotypic 3D tumor spheroid (HTS) models have been receiving increasing attention and come to be widely employed in preclinical studies. The present study is focused on the generation of homotypic (A549 and MDA-MB-231, separately) and heterotypic (A549 + NIH/3T3; MDA-MB-231 + NIH/3T3) 3D tumor spheroids by using GrowDex® nanofibrillar cellulosic (NFC) hydrogel as the scaffold. Light microscopic observations and F-actin staining confirmed the formation of spheroids. The proliferation efficiency indicated an expansion of cell population and an increase in spheroid size over time. The distribution, interaction pattern and influence of fibroblasts on the epithelial cell types were observed in terms of the size and shape of the HTS against homo-spheroids. An interesting observation was that, with an increase in the size of HTSs, many more fibroblast cells were found to occupy the core region, which, perhaps, was due to the faster growth of tumor cells over normal cells. Thus, normal and tumor cells, especially with origins from two different species, can be cultured together in 3D format, and this can potentially enhance our knowledge of tumor microenvironments and cell-cell interaction. These spheroids could

be used to improve microphysiological systems for drug discovery and to better understand the tumor microenvironment.

Keywords: 3D culture; multicellular tumor spheroids; GrowDex®; hydrogel; heterotypic spheroids

1. Introduction

In recent times, there has been a great shift toward using 3D cultures for *in vitro* toxicity testing and drug discovery [1]. Importantly, 3D cell culture models better represent the complex environment and architecture of tumors [2,3]. Although 3D cell models can be produced in hanging drop preparations, most of the models were produced by adopting various scaffolds. Hydrogels are attractive scaffolds that provide structural support to cells and allow them to grow in the 3D format. The use of a hydrogel to fabricate tumor spheroids offers a remarkable advantage over other scaffolds, as it can develop the extracellular matrix (ECM) to achieve realistic cellular responses, especially in the context of disease conditions. The network of interconnected pores present in the hydrogel enable retention of a high water content and facilitate the efficient transport of oxygen, nutrients and waste products [4]. The nanofibrillar cellulose (NFC) hydrogel GrowDex® is ideal for tissue engineering applications considering its intrinsic properties, such as high viscosity, even at low concentrations, non-toxicity, non-animal origins, tunability and having a nano-structure [5,6]. Importantly, it does not require a cross-linker, and it can form a hydrogel even at low concentrations, typically down to 0.1–0.2 wt% [7]. Advantageously, GrowDex® hydrogel possesses a storage modulus close to 10 Pa at 0.5 wt%, which is suitable for the culture of soft tissues. In addition, the spontaneous gelation after shearing imparts the necessary mechanical support for both cell growth and differentiation. It has been successfully used to generate functional spheroids of several normal and cancer cells and stem cell types [8,9]. The HepG2 and HepaRG 3D spheroids thus generated are comparable to those produced using other commercially available hydrogel materials, such as Extracel™, HydroMatrix™ and PuraMatrix™ [7]. In this background, the present study focused on generating spheroids of A549 non-small cell lung cancer cells and MDA-MB-231 metastatic breast cancer cells by using GrowDex® hydrogel for the first time. The morphologies of the spheroids and their F-actin structure were analyzed. The difference in proliferation between spheroid culture and monolayer culture was also studied.

Further, A549 and MDA-MB-231 types of cancer cells were co-cultured with normal mouse embryonic fibroblast cells (NIH/3T3) to focus on the potential of this hydrogel to accommodate multiple cell types, i.e., not only human, but cross-species. Different cell types co-cultured together in direct cell-cell contact mode facilitate cell-cell and cell-microenvironment interactions, which can give further insight into the cellular behavior [10–12]; additionally, the stromal cell types can support the enhanced functional maintenance and phenotype of the target cell types by providing a microenvironment similar to the tissue [12,13]. The idea behind the co-culture of a murine cell with human cells was to create heterotypic tumor spheroids (HTSs). The NIH/3T3 cell type has been used as a cancer-associated fibroblast in several studies [14–17]. Thus, in this study, we integrated nanocellulosic GrowDex® as the hydrogel, A549 non-small cell lung carcinoma and MDA-MB-231 triple-negative breast carcinoma cells as tumor cells and murine NIH/3T3 as the stromal cell to make HTSs and characterize them.

2. Materials and methods

2.1. Cell lines and culture

A549, MDA-MB-231, and NIH/3T3 were procured from the National Center for Cell Science in Pune, India. The cells were maintained and cultured in a DMEM high-glucose medium (Sigma-Aldrich, USA), supplemented with 10% fetal bovine serum (Invitrogen, Bangalore, India) and subjected to 20 mL of penicillin and streptomycin as antibiotics (HyClone, GE Life Sciences) at 37 °C in a humidified atmosphere of 5% CO₂ in a CO₂ incubator (Thermo Scientific, USA). For all cell lines, the medium was renewed every 2nd or 3rd day.

2.2. Spheroid formation

GrowDex® was gifted from UPM Kymmene Corporation in Finland. The hydrogel for the 3D spheroid culture was prepared according to the manufacturer's instructions. Briefly, the stock solution was diluted by using a culture medium to obtain the working concentration. The cells for the 3D culture were prepared as typical for a standard monolayer cell culture. Following trypsinization, 1×10^5 cells were mixed with working GrowDex® hydrogel to obtain approximately 1000 cells/µL in 0.5% GrowDex®. The mixture of cell–hydrogel was added to the agarose pre-coated 24-well culture plates. This agarose coating was applied to prevent attachment of cells to the culture vessel and promote formation of the spheroids.

The growth medium, at volume equal to cell–hydrogel, was added to the top of the cell–hydrogel mixture and incubated at 37 °C and 5% CO₂. The medium was changed once every two days, without disturbing the culture. In order to perform the 2D cell culture, 5.2×10^4 cells were seeded in the wells of 24-well plates and incubated under the same conditions as those for the 3D culture, but the wells were not pre-coated with agarose.

2.3. Light microscopy observation of spheroids

The formation of spheroids was monitored by using an inverted microscope (Axiovert 40 CFL, Carl Zeiss, Jena, Germany) and images were acquired on Days 3, 6 and 10. The morphology of the spheroids was assigned to four categories, i.e., round, mass, grape-bunch-like and stellate, according to Edmondson et al. [18]. Diameters of not less than 10 spheroids were measured by using Carl Zeiss Zen 2012 software, and the average diameter was calculated.

2.4. F-actin staining

The structure of filamentous actin was characterized by performing phalloidin staining. Briefly, the cultured spheroids were fixed in 4% paraformaldehyde for 15 min at 4 °C, washed with phosphate-buffered saline (PBS), permeabilized with 0.1% Triton X-100 and incubated overnight with Alexa Fluor® 532-labeled phalloidin (Thermo-Fisher) to stain the filamentous actin. The spheroids were then counterstained with Hoechst 33258 (Sigma-Aldrich, USA) and observed under a fluorescent microscope (Axioscope 2 Plus, Carl Zeiss, Jena, Germany).

2.5. Analysis of cell viability and proliferation

2.5.1. MTT assay

An MTT [3-(4, 5-Dimethylthiazol-2-yl)-2, 5-Diphenyltetrazolium Bromide] assay was used to measure the difference in proliferation between the 2D and 3D cultures. The protocol of Mosmann [19], with slight modification, was applied. Briefly, at specific intervals (Days 3, 6 and 10), 50 μ L of MTT (Himedia, Mumbai, India) solution (5 mg/mL) was added to the wells of a 24-well plate in which the spheroids were grown. After 3 h of incubation, the spheroids were centrifuged at 1000 rpm for 3–4 min to collect the pellets. One milliliter of dimethyl hydroxide (DMSO) solution was added to the pellets to dissolve the formazan crystals. To measure the absorbance, 200 μ L of the solution was transferred to a 96-well plate. Similarly, for the 2D culture, 50 μ L of the MTT solution was added to each well of the 24-well plate and incubated for 3 h. After incubation, 1 mL of DMSO solution, as above, was added to each well to dissolve the formazan crystals, and 200 μ L of the solution was transferred to a 96-well plate. The absorbance was measured by applying a plate reader at 570 nm, with 630 nm as a reference (iMark, Bio-Rad, USA). The experiments were performed in triplicate, and the mean optical density (OD) was plotted against the days of incubation to evaluate the proliferation efficiency.

2.5.2. DNA quantification assay

In addition to an MTT assay, the proliferation efficiency of the cells in the 2D and 3D cultures was quantitatively analyzed by performing gDNA measurements using the GenEluteTM genomic DNA isolation kit. Briefly, according to the manufacturer's protocol, cells collected on Days 3, 6 and 10 were lysed, pooled and processed. The extracted gDNA was measured by using a UV-vis spectrometer (GeneQuant-1330, Bio-Rad, USA). The experiment was repeated three times, and the mean OD was used to measure the efficacy of the proliferation.

2.6. Generation of heterotypic tumor spheroids

The heterotypic 3D cell culture system was generated by performing a co-culture of mouse embryo-derived fibroblast cells (NIH/3T3) with either of the tumor cell types, i.e., breast (MDA-MB-231) or lung (A549). Briefly, the HTSs were initiated by mixing the breast and lung cancer cells, separately, with the stromal cells (at a 1: 1 ratio by count) in 1 mL GrowDex[®] (0.5 wt% hydrogel). Totally, 2×10^5 cells were added to each well of a 24-well plate and cultured for 5 days (37 °C, 5% CO₂). Homo-spheroids, without NIH/3T3 cells, were also cultured for 5 days to compare the size of the spheroids. After the incubation period, images of the spheroids were captured by using an inverted microscope (Axiovert 40 CFL, Carl Zeiss, Jena, Germany), and the diameters were measured by using Carl Zeiss Zen 2012 software.

2.6.1. Visualization of cell-cell interaction via fluorescein diacetate (FDA) staining

Further, the distribution and interaction of NIH/3T3 fibroblast cells in relation to the epithelial cancer cells were visualized by pre-staining the NIH/3T3 cells with fluorescein diacetate. Briefly, the

NIH/3T3 cells were incubated in an FDA working solution (15 μ M) (InvitrogenTM, Thermo-Fisher, USA) for 30 min, and the excess stain was removed by washing them with PBS. The pre-stained NIH/3T3 cells were mixed and cultured with the epithelial tumor cells as mentioned above. After 3 days of co-culturing, the spheroids were counterstained with Hoechst 33258 (Sigma-Aldrich, USA) and observed under the fluorescent microscope.

2.7. Statistical analysis

The data were subjected to statistical analysis by using PRISM version 8.02 software (GraphPad Software, La Jolla, CA, USA). The values are presented as mean \pm SD of three experimental replicates. The data on the spheroid diameters were subjected to Dunn's multiple comparison test and one-way analysis of variance (ANOVA) testing, whereas the data on the MTT and DNA quantification assays were subjected to two-way ANOVA and Sidak multiple-comparison testing to find the significance of the difference.

3. Results and discussion

3.1. Morphological features of the spheroids

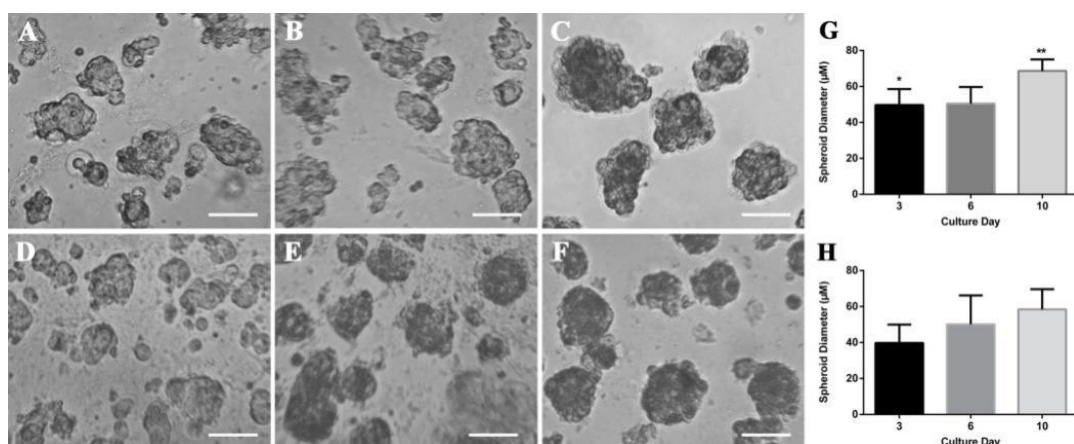


Figure 1. Light microscopy images and diameter measurements of the 3D spheroids. Figure 1A, B and C represent the spheroids of A549, and Figure 1D, E and F represent the spheroids of MDA-MB-231 after Days 3, 6 and 10 of culturing, respectively. The scale bar represents 50 μ m. Figure 1G,H show images of A549 and MDA-MB-231 spheroid diameters, respectively. The error bar represents mean \pm SD (n = 10).

The cancer cells (A549 and MDA-MB-231) are generally polygonal or cuboidal in shape; however, when cultured in GrowDex[®] hydrogel, they formed spheroids (Figure 1). The spheroids of A549 appeared less organized and grape-bunch-like, whereas those of MDA-MB-231 appeared spherical and mass-type. The average diameter of the spheroids, as assessed over a period of time, revealed that the size of the spheroids increased with the passage of time. The diameters of the spheroids of the A549 and MDA-MB-231 cells reached $50 \pm 9 \mu$ m and $50 \pm 16 \mu$ m, respectively, on Day 6, and continued to increase until Day 10. Since the spheroids were small in size, the transport

of oxygen and nutrients to the interior and the removal of CO_2 and metabolic wastes could be achieved via diffusion in the absence of a complex vascular system. When a spheroid grows larger, especially when the diameter is $> 500 \mu\text{m}$, there will be the problem of the limited diffusion of oxygen, nutrients, metabolic waste and soluble factors [20]. Therefore, generally, spheroids with a diameter $< 500 \mu\text{m}$ are recommended for toxicological and biomedical interventions [21]. However, larger spheroids, with cells in the core succumbing to hypoxia and other stresses, offer advantages in terms of studying the effects of the physiochemical gradients on tumor cell characteristics [22,23]. The differences in the morphologies of the spheroids were mainly dependent on the cell lines, the method used to fabricate the spheroids and the physico-mechanical properties of the hydrogel [24,25].

3.2. *F*-actin filaments

The dynamic structure of cellular cytoskeletons is mainly attributable to filamentous actin. It provides structural and functional polarity to the cells and maintains cell-cell communication in tissues [26]. In 2D cultures, the stress fiber of actin tends to cause a decrease in cell-cell contact and subsequent tissue-specific functions [27]. However, the present study revealed densely aggregated F-actin filaments in the cortex and junction of cells grown in the 3D format (Figure 2). The formation of cortical actin bands and junctional F-actin at the points of cell-cell contact have been associated with enhanced cellular adhesion and signal transduction, indicating the preservation of an *in vivo*-like cytoarchitecture in the spheroids [28]. Further, F-actin staining revealed that the A549 spheroids appeared as grape-bunch-like, whereas the MDA-MB-231 spheroids appeared as mass-type.

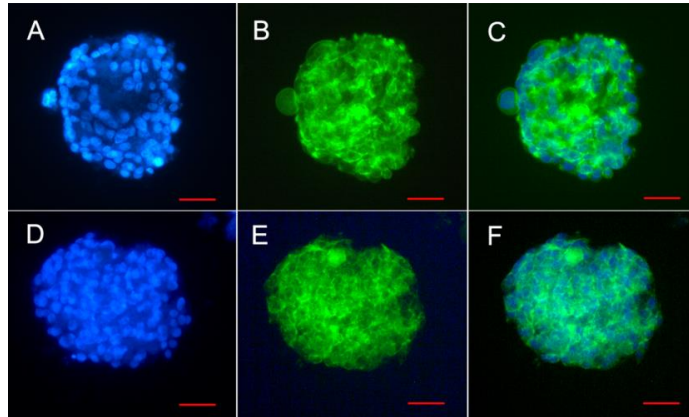


Figure 2. Fluorescence microscopy images of 3D spheroids cultured for 6 days. The left panel (Figure 2A,D) shows the Hoechst counterstained A549 and MDA-MB-231 spheroids (blue color), respectively. The middle panel (Figure 2B,E) represents the F-actin accumulation in the A549 and MDA-MB-231 spheroids, respectively (phalloidin staining; green color). The right panel (Figure 2C,F) represents the merged images of the Hoechst and phalloidin channels, respectively. Scale bar: $50 \mu\text{m}$.

3.3. Difference in proliferation between the 2D and spheroid cultures

Differences in the proliferation of the 2D and spheroid cultures were measured by performing an MTT assay. The results indicated that GrowDex[®] is not cytotoxic to A549 and MDA-MB-231

cells; rather, it facilitates cell proliferation (Figure 3). Throughout the culture, the proliferation of the cells in the 3D format increased gradually, despite the cells having been continuously cultured for 10 days. But, in the 2D culture, the viability was very high on Day 3 and, thereafter, there was a steep decline toward the end of Day 10. The results of the MTT assay are in good agreement with the trend of genomic DNA quantity (Figure 4).

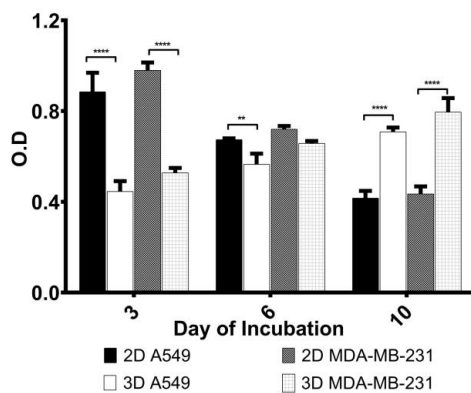


Figure 3. Differences in the cellular proliferation of the 2D culture and 3D spheroids of the A549 and MDA-MB-231 cells at various time points, as revealed by conducting MTT assays. The error bars represent the mean \pm SD ($n = 3$).

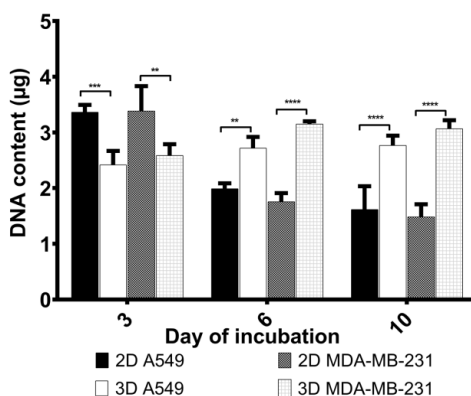


Figure 4. Comparison of cell proliferation between the 2D and 3D cultures of the A549 and MDA-MB-231 cells at various time points, as achieved by quantifying cellular genomic DNA. Significance was tested by performing Tukey's multiple-comparison testing. The error bars represent the mean \pm SD ($n = 3$).

The difference in proliferation between the 3D and 2D cultures, as observed in this study, is consistent with previous findings [29,30]. The results lead to the conclusion that, in the 2D culture, the cells seeded on the plastic surface facing the medium can proliferate and produce progeny only provided there is space, whereas the 3D culture in GrowDex® provided a larger area for cell proliferation all around, resulting in higher cell density and a longer feasible cell culturing duration [31,32]. Importantly, the genes related to cell growth and proliferation were differentially expressed between the 2D and 3D cultures. Especially, the patterns of up-regulated growth-

promoting genes and down-regulated growth-restricting genes were prominent in the 2D-cultured cell lines. Cultures of the same cells in a ECM-mimicking hydrogel environment allows cells to restore the native transcriptional and translational profiles and, thus, maintain the gene expression levels as that observed *in vivo* [29,33,34]. Additionally, the choice of cell line also contributes to change the rate of proliferation [35–37].

3.4. Tumor-stroma cellular interaction as revealed in heterotypic tumor spheroids

Stromal cells in a tumor microenvironment regulate tumor growth, angiogenesis, invasiveness and metastasis by producing growth factors and paracrine or autocrine communication system [38,39]. However, the metabolism of stromal cells can be altered by epithelial cancer cells in a tumor microenvironment. Therefore, studying tumor-stroma interaction is essential to understanding the signaling mechanisms in disease development/progression. To emphasize this, we studied the crosstalk between normal fibroblasts and epithelial cancer cells from the perspectives of spheroid formation and fibroblast distribution.

According to Kapałczyńska et al. [40], cells from different phenotypes do not grow with each other, even in direct co-culture models; it was demonstrated that epithelial cancer cells and fibroblast cells grow according to their own limits. Despite this, the results of FDA staining revealed that, after 3 days of co-culturing, the fibroblast cells were located more in the core of the heterotypic spheroids than at the boundary. The green fluorescence confirms the viability of fibroblast cells from Day 3 of incubation. The observation herein indicates that the fibroblast cells were overpowered by the epithelial cells and fluoresced bright green, whereas the counterstained epithelial cells fluoresced blue (Figure 5). This is an interesting observation, and it provides a basis for future exploration.

Light microscopy observations of the co-culture on Day 6 revealed that the spheroids of the A549 and MDA-MB-231 cells appeared grape-bunch-like and spherical mass type in both the homotypic and heterotypic spheroid formats, and that the cells were tightly packed in the co-cultured spheroids (Figure 6). Importantly, the sizes of the HTSs of the A549 and MDA-MB-231 cells increased by 1.33- and 1.72-fold, respectively, as compared to their respective homotypic counterparts (Figure 5E,F).

It was recorded that the cancer-associated fibroblasts in the 3D co-culture models induced the growth of epithelial cells with a change in the shape of the cells and in the presence of gap junctions and desmosomes, and elevated the expression of neo-vascularization and immune-suppressive growth factors [41–43]. Reports on normal fibroblasts promoting the proliferation of epithelial cancer cells provide contradictory data, with some demonstrating promotion, while others demonstrating the inhibition of epithelial cancer cell growth [44–46]. The size and shape of the heterotypic culture are associated with cell-cell interaction and self-organization of the fibroblasts within the co-cultures [47,48]. The cancer cells grew faster under the conditions of uninhibited cell division, except in the context of contact inhibition on confluence, which is not the case with normal cells. NIH/3T3 cells are not of tumor origin, but are still immortal and contact-inhibited and, therefore, are not normal cells in the strict sense. Therefore, one cell type would not supersede the other. The rate of proliferation and viability after a defined period of incubation in both cases were mainly limited by the culture space available in the monolayer cell culture system [49,50]. A culture of the cells in the 3D format provides much more space than in a monolayer culture because contact inhibition is not a limiting factor in the 3D format.

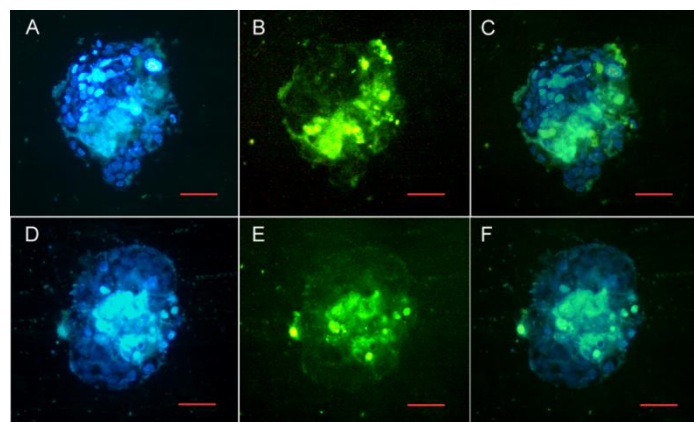


Figure 5. Fluorescence microscopy images of co-cultured spheroids on Day 3 of incubation. The FDA pre-stained NIH/3T3 fibroblast cell was co-cultured with epithelial cell types (A549 and MDA-MB-231). The left panel (Figure 5A,D, respectively) shows images of the Hoechst counterstained A549 and MDA-MB-231 co-cultured spheroids (blue color). The middle panel (Figure 5B,E, respectively) shows images of the FDA pre-stained fibroblast cells (green color) in the co-cultured spheroid of A549 and MDA-MB-23. The right panel (Figure 5C,F, respectively) shows the merged images of the Hoechst and FDA channels. Scale bar: 50 μ m.

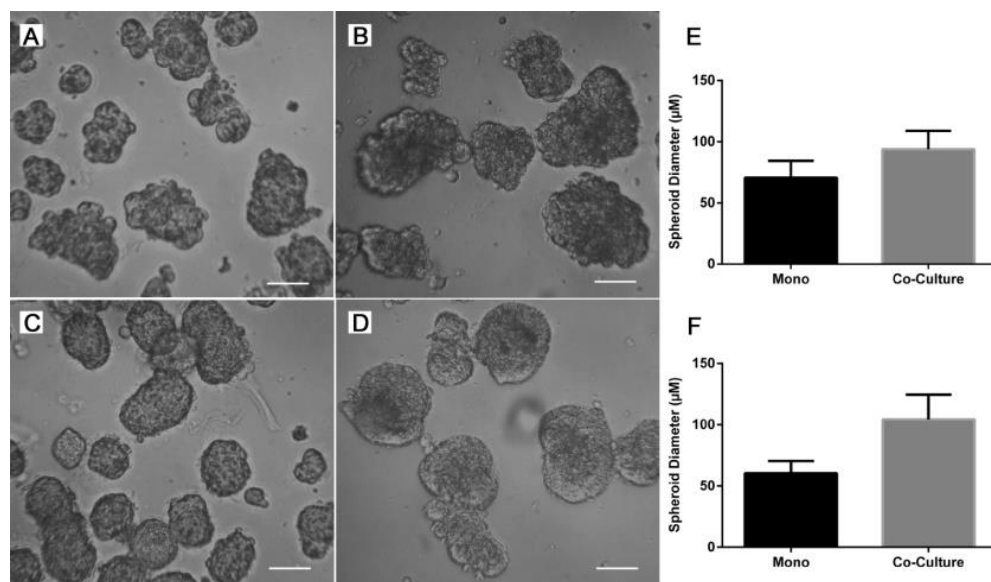


Figure 6. Light microscopy observations of the mono- and co-cultured spheroids on Day 5 of culture. Figure 6A,C show the mono-spheroids of A549 and MDA-MB-231, respectively. Figure 6B,D show the A549 and MDA-MB-231 cells, respectively, co-cultured with mouse-derived fibroblast cells, as spheroids. Figure 6E,F respectively show histograms of the diameters of the mono- and co-culture spheroids of A549 and MDA-MB-231. The error bars represent the mean \pm SD (n = 11). Scale bar: 50 μ m.

In this study, neither the formation of co-culture spheroids nor the accommodation of fibroblasts in the epithelial cells was found to be affected by species differences. In a study, five different human

fibroblast cell lines used as feeder cells for human corneal epithelial cells produced results comparable to 3T3 cells, indicating that there is no manifestation of species difference [51]. Both the mouse and human embryonic fibroblasts equally enhanced the mouse embryo development [52]. However, it has also been reported that the 3T3-L1 fibroblast from mice does not influence the aromatase enzyme activity of breast carcinoma cells, unlike the cancer-associated stromal cells of human origin [53]. Therefore, an in-depth analysis of species differences in regard to co-culturing human and non-human cells is worthy of focused investigation.

One of the milestone advancements in science is the development of microphysiological systems, which is a culmination, as of now, of stem cell science, especially induced pluripotent stem cells, organs-on-chip, 3D spheroids and organoids. It is believed that microphysiological systems will soon replace animal experiments and also be applied to overcome the limitations of the conventional 2D and 3D cultures in toxicology and biomedical science [54,55]. In this context, our findings on homotypic tumor spheroids and HTSs, as well as the success of cost-effective and agile GrowDex® nanocellulosic hydrogel for their production, will go a long way in the application of *in vitro* technologies for chemical risk assessment and drug discovery.

4. Conclusions

In our study, spheroids of A549 and MDA-MB-231 cells, separately and in combination with mouse-derived NIH/3T3 fibroblasts, were successfully developed by using GrowDex® hydrogel. The nano-structure of GrowDex® provides mechanical space (e.g., viscoelasticity), which is relevant to the ECM, supports the compatible co-existence and growth of human- and mouse-derived cells on the same platform and helps to form spheroids without any additional ECM components. The differences in the sizes, morphologies and distribution patterns of two different cell types demonstrated in the 3D heterotypic culture system warrant further in-depth analysis, which can potentially enhance our knowledge of tumor microenvironments and lay the foundation for an attractive model of drug screening for cancer.

Acknowledgments

This work was carried out at Mahatma Gandhi-Doerenkamp Center for Alternatives to the Use of Animals in Life Science Education, Bharathidasan University, Tiruchirappalli, which was established and is funded by the Doerenkamp-Zbinden Foundation, Switzerland. We thank UPM Biomedicals, Helsinki, Finland, for providing the GrowDex® NFC hydrogel.

Conflict of interest

All authors declare no conflicts of interest regarding this study.

References

1. Caleb J, Young T (2020) Is it time to start transitioning from 2D to 3D cell culture? *Front Mol Biosci* 7: 33. <https://doi.org/10.3389/fmolb.2020.00033>

2. Alzeeb G, Corcos L, Jossic-Corcos CL (2022) Spheroids to organoids: solid cancer models for anticancer drug discovery. *B Cancer* 109: 49–57. <https://doi.org/10.1016/j.bulcan.2021.09.019>
3. Balaji P, Murugadas A, Shanmugaapriya S, et al. (2019) Fabrication and characterization of egg white cryogel scaffold for three-dimensional (3D) cell culture. *Biocatal Agric Biotechnol* 17: 441–446. <https://doi.org/10.1016/j.bcab.2018.12.019>
4. Drury JL, Mooney DJ (2003) Hydrogels for tissue engineering: scaffold design variables and applications. *Biomaterials* 24: 4337–4351. [https://doi.org/10.1016/S0142-9612\(03\)00340-5](https://doi.org/10.1016/S0142-9612(03)00340-5)
5. Shelke NB, James R, Laurencin CT, et al. (2014) Polysaccharide biomaterials for drug delivery and regenerative engineering. *Polym Adv Technol* 25: 448–460. <https://doi.org/10.1002/pat.3266>
6. Joshi MK, Pant HR, Tiwari AP, et al. (2016) Three-dimensional cellulose sponge: fabrication, characterization, biomimetic mineralization, and *in vitro* cell infiltration. *Carbohydr Polym* 136: 154–162. <https://doi.org/10.1016/j.carbpol.2015.09.018>
7. Bhattacharya M, Malinen MM, Lauren P, et al. (2012) Nanofibrillar cellulose hydrogel promotes three-dimensional liver cell culture. *J Control Release* 164: 291–298. <https://doi.org/10.1016/j.jconrel.2012.06.039>
8. Lou YR, Kanninen L, Kuisma T, et al. (2014) The use of nanofibrillar cellulose hydrogel as a flexible three-dimensional model to culture human pluripotent stem cells. *Stem Cells Dev* 23: 380–392. <https://doi.org/10.1089/scd.2013.0314>
9. Malinen MM, Kanninen LK, Corlu A, et al. (2014) Differentiation of liver progenitor cell line to functional organotypic cultures in 3D nanofibrillar cellulose and hyaluronan-gelatin hydrogels. *Biomaterials* 35: 5110–5121. <https://doi.org/10.1016/j.biomaterials.2014.03.020>
10. Kawada H, Ando K, Tsuji T, et al. (1999) Rapid ex vivo expansion of human umbilical cord hematopoietic progenitors using a novel culture system. *Exp Hematol* 27: 904–915. [https://doi.org/10.1016/S0301-472X\(99\)00012-0](https://doi.org/10.1016/S0301-472X(99)00012-0)
11. Yamamoto Y, Mochida J, Sakai D, et al. (2004) Upregulation of the viability of nucleus pulposus cells by bone marrow-derived stromal cells: significance of direct cell-to-cell contact in coculture system. *Spine* 29: 1508–1514. <https://doi.org/10.1097/01.brs.0000131416.90906.20>
12. Paschos NK, Brown WE, Eswaramoorthy R, et al. (2015) Advances in tissue engineering through stem cell-based co-culture. *J Tissue Eng Regen M* 9: 488–503. <https://doi.org/10.1002/term.1870>
13. Hendriks J, Riesle J, van Blitterswijk CA (2007) Co-culture in cartilage tissue engineering. *J Tissue Eng Regen M* 1: 170–178. <https://doi.org/10.1002/term.19>
14. Saito RA, Micke P, Paulsson J, et al. (2010) Forkhead box F1 regulates tumor-promoting properties of cancer-associated fibroblasts in lung cancer. *Cancer Res* 70: 2644–2654. <https://doi.org/10.1158/0008-5472.CAN-09-3644>
15. Thoma CR, Stroebel S, Rösch N, et al. (2013) A high-throughput-compatible 3D microtissue co-culture system for phenotypic RNAi screening applications. *J Biomol Screen* 18: 1330–1337. <https://doi.org/10.1177/1087057113499071>
16. Thoma CR, Zimmermann M, Agarkova I, et al. (2014) 3D cell culture systems modeling tumor growth determinants in cancer target discovery. *Adv Drug Deliver Rev* 69–70: 29–41. <https://doi.org/10.1016/j.addr.2014.03.001>
17. Rama-Esendagli D, Esendagli G, Yilmaz G, et al. (2014) Spheroid formation and invasion capacity are differentially influenced by co-cultures of fibroblast and macrophage cells in breast cancer. *Mol Biol Rep* 41: 2885–2892. <https://doi.org/10.1007/s11033-014-3144-3>

18. Edmondson R, Broglie JJ, Adcock AF, et al. (2014) Three-dimensional cell culture systems and their applications in drug discovery and cell-based biosensors. *Assay Drug Dev Technol* 12: 207–218. <https://doi.org/10.1089/adt.2014.573>
19. Mosmann T (1983) Rapid colorimetric assay for cellular growth and survival: application to proliferation and cytotoxicity assays. *J Immunol Methods* 65: 55–63. [https://doi.org/10.1016/0022-1759\(83\)90303-4](https://doi.org/10.1016/0022-1759(83)90303-4)
20. Groebe K, Mueller-Klieser W (1991) Distributions of oxygen, nutrient, and metabolic waste concentrations in multicellular spheroids and their dependence on spheroid parameters. *Eur Biophys J* 19: 169–181. <https://doi.org/10.1007/BF00196343>
21. Zanoni M, Piccinini F, Arienti C, et al. (2016) 3D tumor spheroid models for *in vitro* therapeutic screening: a systematic approach to enhance the biological relevance of data obtained. *Sci Rep UK* 6: 19103. <https://doi.org/10.1038/srep19103>
22. Mehta G, Hsiao AY, Ingram M, et al. (2012) Opportunities and challenges for use of tumor spheroids as models to test drug delivery and efficacy. *J Control Release* 164: 192–204. <https://doi.org/10.1016/j.conrel.2012.04.045>
23. Nath S, Devi GR (2016) Three-dimensional culture systems in cancer research: focus on tumor spheroid model. *Pharmacol Therapeut* 163: 94–108. <https://doi.org/10.1016/j.pharmthera.2016.03.013>
24. Lin RZ, Chang HY (2008) Recent advances in three-dimensional multicellular spheroid culture for biomedical research. *Biotechnol J* 3: 1172–1184. <https://doi.org/10.1002/biot.200700228>
25. Weiss MS, Bernabé BP, Shikanov A, et al. (2012) The impact of adhesion peptides within hydrogels on the phenotype and signaling of normal and cancerous mammary epithelial cells. *Biomaterials* 33: 3548–3559. <https://doi.org/10.1016/j.biomaterials.2012.01.055>
26. Chu YS, Thomas WA, Eder O, et al. (2004) Force measurements in E-cadherin-mediated cell doublets reveal rapid adhesion strengthened by actin cytoskeleton remodeling through Rac and Cdc42. *J Cell Biol* 167: 1183–1194. <https://doi.org/10.1083/jcb.200403043>
27. Abu-Absi SF, Friend JR, Hansen LK, et al. (2002) Structural polarity and functional bile canaliculi in rat hepatocyte spheroids. *Exp Cell Res* 274: 56–67. <https://doi.org/10.1006/excr.2001.5467>
28. Zhang J, Betson M, Erasmus J, et al. (2005) Actin at cell-cell junctions is composed of two dynamic and functional populations. *J Cell Sci* 118: 5549–5562. <https://doi.org/10.1242/jcs.02639>
29. Gurski LA, Petrelli NJ, Jia X, et al. (2010) 3D Matrices for anti-cancer drug testing and development. *Oncol Issues* 25: 20–25. <https://doi.org/10.1080/10463356.2010.11883480>
30. Khaitan D, Chandna S, Arya MB, et al. (2006) Establishment and characterization of multicellular spheroids from a human glioma cell line; implications for tumor therapy. *J Transl Med* 4: 12. <https://doi.org/10.1186/1479-5876-4-12>
31. Basu S, Yang ST (2005) Astrocyte growth and glial cell line-derived neurotrophic factor secretion in three-dimensional polyethylene terephthalate fibrous matrices. *Tissue Eng* 11: 940–952. <https://doi.org/10.1089/ten.2005.11.940>
32. Luo J, Yang ST (2004) Effects of three-dimensional culturing in a fibrous matrix on cell cycle, apoptosis, and MAb production by hybridoma cells. *Biotechnol Progr* 20: 306–315. <https://doi.org/10.1021/bp034181v>

33. Birgersdotter A, Sandberg R, Ernberg I (2005) Gene expression perturbation *in vitro*—a growing case for three-dimensional (3D) culture systems. *Semin Cancer Biol* 15: 405–412. <https://doi.org/10.1016/j.semcan.2005.06.009>

34. Kenny PA, Lee GY, Myers CA, et al. (2007) The morphologies of breast cancer cell lines in three-dimensional assays correlate with their profiles of gene expression. *Mol Oncol* 1: 84–96. <https://doi.org/10.1016/j.molonc.2007.02.004>

35. Park JS, Woo DG, Sun BK, et al. (2007) *In vitro* and *in vivo* test of PEG/PCL-based hydrogel scaffold for cell delivery application. *J Control Release* 124: 51–59. <https://doi.org/10.1016/j.jconrel.2007.08.030>

36. Semino CE, Merok JR, Crane CG, et al. (2003) Functional differentiation of hepatocyte-like spheroid structures from putative liver progenitor cells in three-dimensional peptide scaffolds. *Differentiation* 71: 262–270. <https://doi.org/10.1046/j.1432-0436.2003.7104503.x>

37. Wang X, Sun L, Maffini MV, et al. (2010) A complex 3D human tissue culture system based on mammary stromal cells and silk scaffolds for modeling breast morphogenesis and function. *Biomaterials* 31: 3920–3929. <https://doi.org/10.1016/j.biomaterials.2010.01.118>

38. Pageau SC, Sazonova OV, Wong JY, et al. (2011) The effect of stromal components on the modulation of the phenotype of human bronchial epithelial cells in 3D culture. *Biomaterials* 32: 7169–7180. <https://doi.org/10.1016/j.biomaterials.2011.06.017>

39. Shen FH, Werner BC, Liang H, et al. (2013) Implications of adipose-derived stromal cells in a 3D culture system for osteogenic differentiation: an *in vitro* and *in vivo* investigation. *Spine J* 13: 32–43. <https://doi.org/10.1016/j.spinee.2013.01.002>

40. Kapałczyńska M, Kolenda T, Przybyła W, et al. (2018) 2D and 3D cell cultures—a comparison of different types of cancer cell cultures. *Arch Med Sci* 14: 910–919. <https://doi.org/10.5114/aoms.2016.63743>

41. Khawar LA, Park JK, Jung ES, et al. (2018) Three dimensional mixed-cell spheroids mimic stroma-mediated chemoresistance and invasive migration in hepatocellular carcinoma. *Neoplasia* 20: 800–812. <https://doi.org/10.1016/j.neo.2018.05.008>

42. Mishra P, Banerjee D, Ben-Baruch A (2011) Chemokines at the crossroads of tumor-fibroblast interactions that promote malignancy. *J Leukocyte Biol* 89: 31–39. <https://doi.org/10.1189/jlb.0310182>

43. Tyan SW, Kuo WH, Huang CK, et al. (2011) Breast cancer cells induce cancer-associated fibroblasts to secrete hepatocyte growth factor to enhance breast tumorigenesis. *Plos One* 6: e15313. <https://doi.org/10.1371/journal.pone.0015313>

44. Sacco AJ, Ricciardelli C, Mayne K, et al. (2001) Versican accumulation in human prostatic fibroblast cultures is enhanced by prostate cancer cell-derived transforming growth factor β 1. *Cancer Res* 61: 926–930.

45. Wernert N, Kaminski A, Haddouti EM, et al. (2007) Tumor-stroma interactions of metastatic prostate cancer cell lines, In: Rampal, J.B., *Methods in Molecular Biology*, Humana Press, 223–237. https://doi.org/10.1007/978-1-59745-304-2_14

46. O'Connor JC, Farach-Carson MC, Schneider CJ, et al. (2007) Coculture with prostate cancer cells alters endoglin expression and attenuates transforming growth factor- β signaling in reactive bone marrow stromal cells. *Mol Cancer Res* 5: 585–603. <https://doi.org/10.1158/1541-7786.MCR-06-0408>

47. Howes AL, Richardson RD, Finlay D, et al. (2014) 3-Dimensional culture systems for anti-cancer compound profiling and high-throughput screening reveal increases in EGFR inhibitor-mediated cytotoxicity compared to monolayer culture systems. *Plos One* 9: e108283. <https://doi.org/10.1371/journal.pone.0108283>
48. Jaganathan H, Gage J, Leonard F, et al. (2014) Three-dimensional *in vitro* co-culture model of breast tumor using magnetic levitation. *Sci Rep-UK* 4: 6468. <https://doi.org/10.1038/srep06468>
49. Levine EM, Jeng DY, Chang Y (1974) Contact inhibition, polyribosomes, and cell surface membranes in cultured mammalian cells. *J Cell Physiol* 84: 349–363. <https://doi.org/10.1002/jcp.1040840304>
50. Schmialek P, Geyer A, Miosga V, et al. (1977) The kinetics of contact inhibition in mammalian cells. *Cell Proliferat* 10: 195–202. <https://doi.org/10.1111/j.1365-2184.1977.tb00144.x>
51. Lu R, Bian F, Lin J, et al. (2012) Identification of human fibroblast cell lines as a feeder layer for human corneal epithelial regeneration. *Plos One* 7: e38825. <https://doi.org/10.1371/journal.pone.0038825>
52. Nematollahi-mahani SN, Pahang H, Moshkdanian G, et al. (2009) Effect of embryonic fibroblast cell co-culture on development of mouse embryos following exposure to visible light. *J Assist Reprod Gen* 26: 129–135. <https://doi.org/10.1007/s10815-008-9290-6>
53. Miki Y, Suzuki T, Tazawa C, et al. (2007) Aromatase localization in human breast cancer tissues: possible interactions between intratumoral stromal and parenchymal cells. *Cancer Res* 67: 3945–3954. <https://doi.org/10.1158/0008-5472.CAN-06-3105>
54. Akbarsha MA, Balaji P, Shanmugaapriya S (2022) Multicellular spheroid culture using egg white as an economically viable platform for application in microphysiological systems, *New Orleans, Abstracts of the 1st Microphysiological Systems World Summit*, 17. https://mpsworldsummit.com/wp-content/uploads/2022/05/altex_MPS1.pdf
55. Rowan A, New technology, better science, and fewer animals, 2022. Available from: <https://wellbeingintl.org/new-technology-better-science-and-fewer-animals/>.



AIMS Press

© 2022 the Author(s), licensee AIMS Press. This is an open access article distributed under the terms of the Creative Commons Attribution License (<http://creativecommons.org/licenses/by/4.0>)